Southern Ocean acidification: A tipping point at 450-ppm atmospheric CO_2

Ben I. McNeil[a,1] and Richard J. Matear[b]

[a]Climate Change Research Centre, Faculty of Science, University of New South Wales, Sydney NSW 2052, Australia; and [b]Centre for Australian Weather and Climate Research and Antarctic Climate & Ecosystems Cooperative Research Centre, Hobart TAS 7000, Australia

Edited by David M. Karl, University of Hawaii, Honolulu, HI, and approved October 6, 2008 (received for review July 1, 2008)

Southern Ocean acidification via anthropogenic CO_2 uptake is expected to be detrimental to multiple calcifying plankton species by lowering the concentration of carbonate ion (CO_3^{2-}) to levels where calcium carbonate (both aragonite and calcite) shells begin to dissolve. Natural seasonal variations in carbonate ion concentrations could either hasten or dampen the future onset of this undersaturation of calcium carbonate. We present a large-scale Southern Ocean observational analysis that examines the seasonal magnitude and variability of CO_3^{2-} and pH. Our analysis shows an intense wintertime minimum in CO_3^{2-} south of the Antarctic Polar Front and when combined with anthropogenic CO_2 uptake is likely to induce aragonite undersaturation when atmospheric CO_2 levels reach ≈450 ppm. Under the IPCC IS92a scenario, Southern Ocean wintertime aragonite undersaturation is projected to occur by the year 2030 and no later than 2038. Some prominent calcifying plankton, in particular the Pteropod species *Limacina helicina*, have important veliger larval development during winter and will have to experience detrimental carbonate conditions much earlier than previously thought, with possible deleterious flow-on impacts for the wider Southern Ocean marine ecosystem. Our results highlight the critical importance of understanding seasonal carbon dynamics within all calcifying marine ecosystems such as continental shelves and coral reefs, because natural variability may potentially hasten the onset of future ocean acidification.

carbon cycle | climate change

Oceanic absorption of anthropogenic CO_2 has lowered the pH and concentration of carbonate ion (CO_3^{2-}) substantially since preindustrial times (1–3). These changes, particularly with respect to carbonate ion, strongly vary between ocean basins. Over the 21st century, the carbonate ion levels over most of the surface ocean are expected to remain supersaturated with respect to aragonite (2, 3), the more soluble form of calcium carbonate. Despite this, studies have demonstrated that calcifying organisms depend on variations in aragonite saturation state (3–5). Aragonite saturation in seawater allows marine organisms to adequately secrete and accumulate this carbonate mineral during growth and development. The Southern Ocean (south of 60°S), however, is predicted to begin to experience aragonite undersaturation by the year 2050 if assuming surface ocean CO_2 equilibrium with the atmosphere, while most ocean models suggest that mean surface conditions throughout the Southern Ocean will become undersaturated by the year 2100 (3). Aragonite undersaturation both enhances the dissolution of aragonite and reduces formation of aragonite shells of marine organisms (4–7), making the prediction of aragonite undersaturation by the end of this century of particular concern to the Southern Ocean marine ecosystem. Systematic natural seasonal variations of pH and CO_3^{2-} can either amplify or depress the onset of future ocean acidification and aragonite undersaturation. Although seasonal variability has been suggested to hasten the onset of aragonite undersaturation (3), observational evidence in the Southern Ocean has been lacking.

Results and Discussion

Here we reconstruct the Southern Ocean seasonal cycle of pH and CO_3^{2-} for the nominal year of 1995 by employing an empirical data analysis of all available carbon measurements (8). To test the realism of our empirical data reconstructions, we analyze wintertime measurements that were not used in the empirical analysis [see supporting information (SI) *Text*]. Our empirical data reconstructions compare well to the direct observations and show a strong wintertime minimum south of 60°S for CO_3^{2-} (Figs. 1 and 2). Winter cooling along with strong persistent winds combine to ventilate deeper waters in the Southern Ocean south of the Polar Front. These Southern Ocean deep waters are rich in dissolved inorganic carbon (DIC) but are carbonate-poor, and the entrainment of these waters into the surface layer lowers the carbonate ion concentration considerably. An analysis of the components driving Southern Ocean seasonal carbon variability shows upwelling of carbonate-deplete deep waters to be the most dominant driver of wintertime carbon cycling in comparison to solubility or biological processes (8). During summertime, shallow mixed layers evolve where biological production depletes DIC and enriches carbonate ion concentrations driving substantial seasonal variability. Our results show strong variations in the seasonal amplitude of pH and CO_3^{2-} where some Southern Ocean regions undergo annual variability of up to 35 μmol/kg for CO_3^{2-} and 0.06 for pH (Fig. 2). This level of natural seasonal variability has large implications for the onset of future ocean acidification within the Southern Ocean.

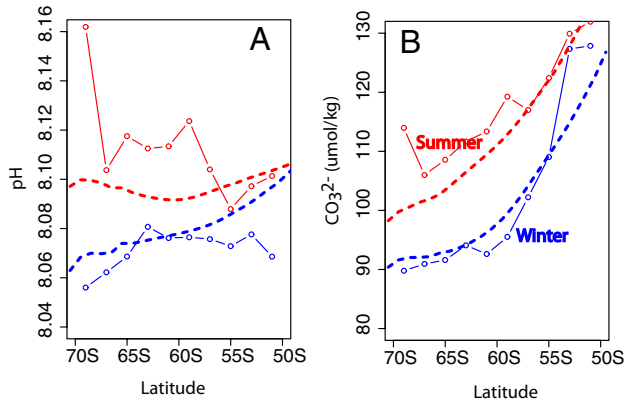

Fig. 1. Zonally averaged surface carbon measurements for the Southern Ocean where blue represents wintertime conditions (April–October) and red represents summertime conditions (November–March). Solid lines with circles represent the raw measurements from the Global Ocean Data Analysis Project database (12), and the dotted lines represent the empirical prediction from this study. (*A*) pH. (*B*) Carbonate ion (CO_3^{2-}, μmol/kg). For reference, the carbonate ion concentration for aragonite saturation is ≈65 μmol/kg.

Author contributions: B.I.M. designed research; R.J.M. and B.I.M. performed research; B.I.M. analyzed data; and B.I.M. wrote the paper.

The authors declare no conflict of interest.

This article is a PNAS Direct Submission.

[1]To whom correspondence should be addressed. E-mail: b.mcneil@unsw.edu.au.

This article contains supporting information online at www.pnas.org/cgi/content/full/0806318105/DCSupplemental.

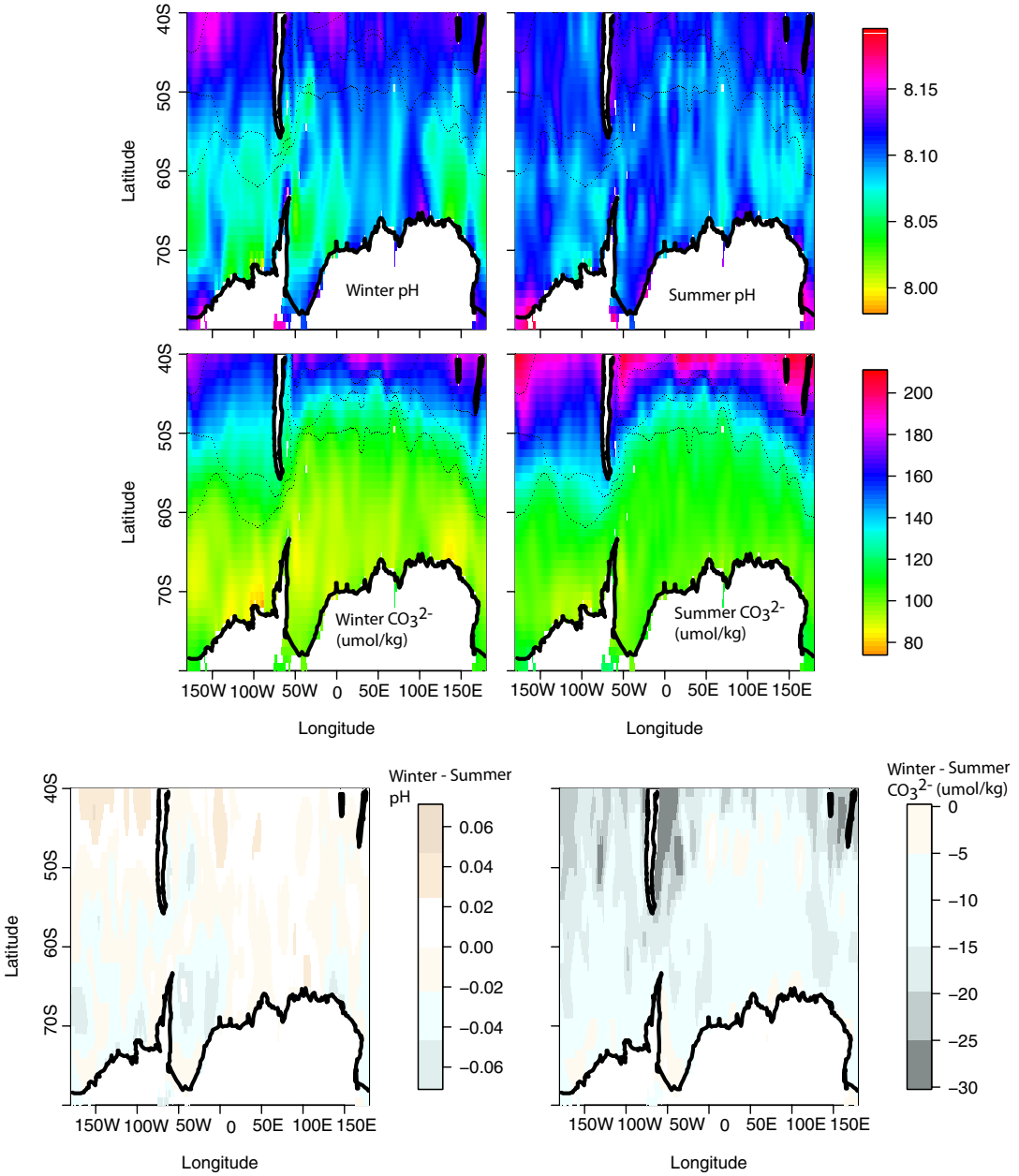

Fig. 2. Seasonal estimates of pH and CO_3^{2-} for the Southern Ocean. (*Top*) Winter and summer distributions of pH. (*Middle*) Winter and summer distributions of CO_3^{2-}. (*Bottom*) Surface contour map of the seasonal amplitude (winter–summer) from the empirically derived values from this study of pH and carbonate ion (CO_3^{2-}, μmol/kg).

Assuming that the observed seasonal amplitude does not change over the coming decades, we can use this new information to better determine the onset of future aragonite undersaturation in the Southern Ocean. The new reconstructed seasonal cycle allows some important advances in projecting future ocean acidification and the onset of aragonite undersaturation state in the Southern Ocean. First, our reconstructed annual cycle in the year 1995 can be used as the starting point, instead of needing to calculate CO_2 equilibrium conditions since preindustrial times. By using our starting point from the observed annual cycle for 1995 derived here, we implicitly correct for any preexisting atmosphere–ocean CO_2 disequilibrium biases in the Southern Ocean since preindustrial times (9). Second, we estimate the future Southern Ocean CO_2 disequilibrium bias from the year 1995 using an ocean carbon model (2, 3) with prescribed IS92a atmospheric CO_2 concentrations instead of relying on absolute model projections for future ocean acidification. Third, an inherent bias has been found recently when truncating important nutrient variations in the definition of alkalinity (10), which adds a small but consistent bias in the Southern Ocean when projecting future ocean acidification from models. Our data-constrained future ocean acidification projections fully take into account these nutrient variations in the estimate of total alkalinity. Climate change feedbacks such as ocean warming, deep-water ventilation changes, and sea-ice melt potentially alter future surface ocean carbonate conditions. Previous work has shown climate change feedbacks to slightly increase the level of surface carbonate ion, due to warming invoking solubility-driven CO_2 out-gassing from the ocean (2, 3). In the Southern Ocean, however, these changes were found to be insignificant as the

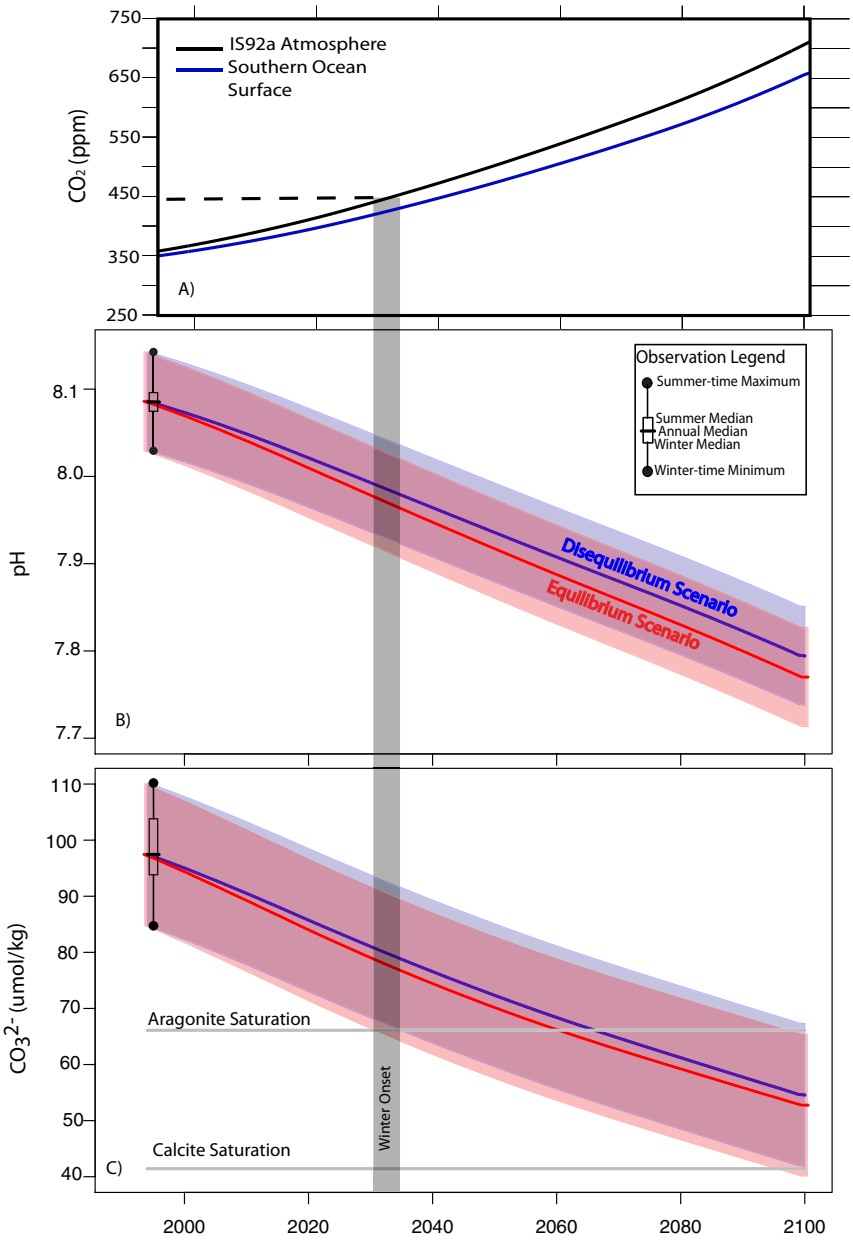

Fig. 3. Observed and predicted Southern Ocean surface acidification conditions for the 21st century. (*A*) IPCC IS92a atmospheric CO_2 scenario (black) and the average oceanic pCO_2 level south of 60°S from the CSIRO ocean carbon model (blue line). (*B* and *C*) Projections for Southern Ocean (south of 60°S) for surface pH and carbonate ion (CO_3^{2-}, μmol/kg) for two different methods using the IPCC IS92a atmospheric CO_2 scenario. The observed seasonal cycle is represented in the year 1995 with a box-and-whiskers plot. The concentration of CO_3^{2-} that results in aragonite and calcite saturation is shown by the horizontal dotted lines. The observations were used as the baseline for these two different scenarios. The solid red line represents the average conditions assuming atmospheric equilibrium from the year 1995, and the blue line includes the estimated CO_2 disequilibrium from the CSIRO climate model. The shading for red and blue represents the maximum seasonal variability taken from the observations derived here.

surface ocean is projected to move toward CO_2 equilibrium via local changes in upwelling and sea-ice melt, which more than offsets the higher carbonate concentrations from ocean warming (2). Hence, our projections neglect the impact of climate change impacts on Southern Ocean acidification.

Diagnosing future ocean acidification has relied on annual average equilibrium calculations and/or ocean model predictions that suggest aragonite undersaturation to start as early as 2050 and up until the year 2100 (1–3, 11). Our results show wintertime aragonite undersaturation to potentially begin once atmospheric CO_2 concentration reaches 450 ppm, which is the year 2030 using the IPCC IS92a scenario (Figs. 3 and 4). It must be emphasized, however, that the timeframe for atmospheric CO_2 to reach 450 ppm could be earlier or later depending on the trajectory of future CO_2 emissions. If taking into account average Southern Ocean ocean–atmosphere CO_2 disequilibrium, the onset of wintertime aragonite undersaturation under the IS92a scenario would be the year 2038 (Fig. 3). This means that wintertime undersaturation is projected to begin 30 years before the annual average, which is projected to occur by the year 2060 (Fig. 3).

The onset of wintertime aragonite undersaturation varies among Southern Ocean regions with a tendency for early undersaturation in the latitudinal band between 65 and 70°S, which coincides with the latitudinal band for deep-water up-

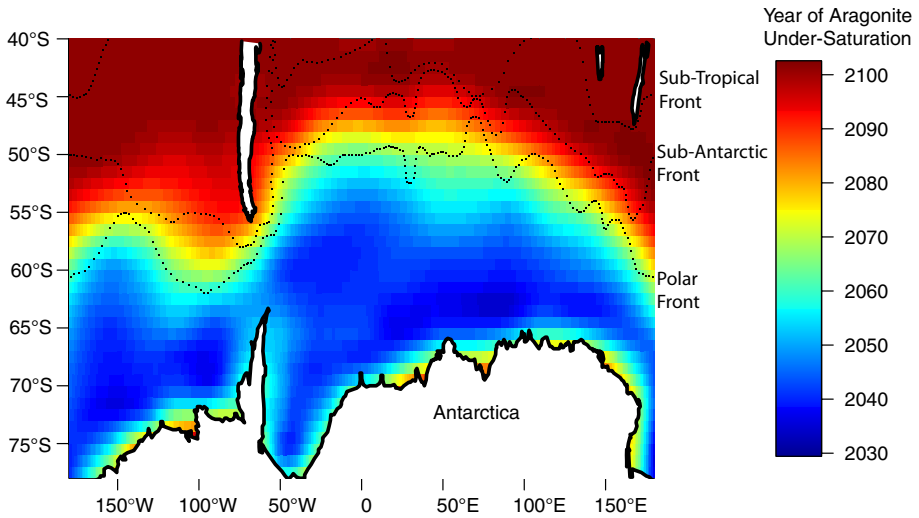

Fig. 4. Contour plot of the year in which the onset of wintertime undersaturation occurs under equilibrium conditions. Shown are the average location of Southern Ocean fronts (38).

welling (Fig. 4). Coinciding elevated summertime carbonate ion concentrations suggest that some regions will continue to be aragonite-saturated in the summertime up until the end of this century (Fig. 3). Unlike previous estimates, the wintertime minimum carbonate ion concentrations in some parts of the Southern Ocean are expected to drive calcite undersaturation (the more stable form of calcium carbonate) by the year 2095 (Fig. 2), several decades before the average onset will occur. Surface ocean pH levels have already been observed to be lowered by ≈0.1 in the Southern Ocean (2, 12) and are projected to decline a further ≈0.3 by the year 2100 (Fig. 3), corresponding to an increase in H^+ concentrations of 150% (1–3). Including the seasonality in pH, this 0.3 pH decline will occur in the winter by the year 2080 (Fig. 3).

Early aragonite undersaturation is of particular concern for the zooplankton species comprising Pteropods, which form aragonite shells. Southern Ocean Pteropods comprise up to one-quarter of total zooplankton biomass in the Ross Sea (13), Weddell Sea (14), and East Antarctica (15), can sometimes displace krill as the dominant zooplankton (16), and dominate carbonate export fluxes south of the Antarctic Polar Front (17), and even organic carbon export (18). Pteropods in Southern Ocean sediment traps show partial dissolution and "frosted" appearance of shells just below the aragonite saturation horizon (17, 19), indicating vulnerability to low carbonate ion concentrations. The most dominant Southern Ocean Pteropod species is *Limacina helicina*, with *Limacina retroversa* and others playing a smaller role (20). The dominant species, *L. helicina*, is known to have a life cycle of 1–2 years with important veliger larval development during winter months (20–22), which will be adversely impacted by early wintertime aragonite undersaturation. Given their multiyear life cycles, our results imply that Pteropods in the Southern Ocean will need to withstand aragonite undersaturation far sooner than previously predicted with possible significant effects throughout the Southern Ocean marine food web.

Our analysis shows a clear distinction at the Antarctic Polar Front between aragonite saturation to the north and early undersaturation to the south (Fig. 4). We find a strong gradient in carbonate ion concentration from 90 to 125 μmol/kg across the modern-day Polar Frontal Zone (Figs. 1 and 2). Biological surveys and sediment trap data reveal that Pteropods are important calcifying plankton south of Polar Front (15, 17, 19, 23). With such contrasting carbonate chemistry between the sub-Antarctic and Antarctic zones, the Polar Frontal Zone would be the optimal location for northward migration of species in response to the rapid undersaturation to the south (3). Frontal surveys investigating zooplankton migration patterns would provide valuable insights into the potential for these species to migrate in the future. Furthermore, our observations show seasonal variations of carbonate up to 25–30 μmol/kg in parts of the Southern Ocean (Fig. 2). These large seasonal variations in carbonate ion are equivalent to the average decline in carbonate ion to the year 2065 via the uptake of anthropogenic CO_2 (IS92a scenario, Fig. 3). Such regions of high carbonate ion variability could also provide important test beds to understand the adaptive resilience of calcifying organisms to aragonite undersaturation.

The implications of our results are not limited to the Southern Ocean. Natural seasonal amplification of anthropogenic oceanic acidification in all ocean basins and coral reef ecosystems will result in delaying or accelerating the onset of detrimental oceanic acidification conditions for a variety of calcifying marine organisms throughout the marine biosphere. Large seasonal variations in carbonate ion have shown to be linked with growth of the calcifying coccolithophore species *Emiliania huxleyi* in the Bering Sea (24) and the Baltic Sea (25). The large seasonal and spatial variability of carbonate ion observed here in the Southern Ocean coupled with recent evidence of upwelling-driven coastal aragonite undersaturation (26) highlights the need for a more robust understanding of seasonal variability in areas important for calcifying organisms, where the timing of detrimental carbonate conditions could be altered dramatically.

Materials and Methods

Empirical Approach to Estimate the Seasonal Cycle of DIC, ALK, pH, and CO_3^{2-}. The empirical approach adopted here is similar to recent methodologies investigating the annual cycle of pCO_2 and air–sea CO_2 fluxes in the Southern Ocean (8) and Indian Ocean (27). All Southern Ocean carbon bottle measurements up to 55-m depth were taken from the CO_2 Survey of the World Ocean Circulation Experiment and the Joint Global Ocean Flux Study. These measurements were made publicly available through the Global Ocean Data Analysis Project and described elsewhere (12). The DIC measurements were collected over more than a decade up to the year 2000. The first step in our approach was therefore to normalize the DIC data to a common year (1995) to account for interannual anthropogenic CO_2 uptake. For the normalization we used the CFC-age technique, which is described elsewhere (28). After normalizing the surface DIC measurements to a common year, a multiple linear least-squares regression was conducted by using various parameters as predictors in a way similar to previous work in other ocean basins (27, 29–31). The regression equation for DIC is represented by

$$\mathrm{DIC}_{\mathrm{obs}} = \alpha_0 + \sum_{i=1}^{n} \alpha_i P_i + \epsilon_i,$$

where α_i are the partial regression coefficients for n independent parameters (P_i), α_0 is the intercept, and ε_I are the residuals. The optimal regression was chosen by maximizing the adjusted coefficient of determination (R^2) while minimizing the standard error of the fit. The final resulting fit, $DIC = 883.9 - 6.6 \times \theta + 37.7 \times Sal - 0.3 \times O_2 + 2.9 \times Nit + 0.3 \times Sil$, was obtained with a standard error of ≈8 μmol/kg and an adjusted R^2 of 0.98 using 1,032 measurements, of which 65% were collected during spring and summer months, the remaining being collected during autumn and winter months (see Fig. S1 for sampling locations). The addition of phosphate as an independent parameter did not improve the fit significantly because of the high covariance with nitrate. To investigate the seasonal dependence we also separated austral summer (November–March) and austral winter (April–October) data and found little change in the DIC fit (8). Surface alkalinity (ALK) has been shown to closely follow the salinity distribution in the Southern Ocean (32–34). We explored empirical predictions of surface ALK and found that the inclusion of salinity, nitrate, and silicate improved the empirical estimations to within 8.1 μmol/kg, described by the equation $ALK = 678.5 + 46.6 \times S + 0.8 \times \mathrm{Nit} + 0.3 \times Sil$, $R^2 = 0.74$, using 1,200 measurements. The World Ocean Atlas climatology for hydrographic parameters was used to extrapolate the DIC and ALK seasonal to a 1 × 1° grid. The pH and CO_3^{2-} were calculated by using optimal CO_2 dissociation constants (35). The pH of seawater is defined by the amount of H^+ ions available: $\mathrm{pH} = -\log_{10}[H^+]$.

Error Analysis. The empirical approach used here to estimate the annual cycle of carbonate system parameters introduces both systematic and random errors. The random errors introduced from our empirical regression methodology were ± 8 μmol/kg for both DIC and ALK, corresponding to a pH uncertainty of ± 0.02 and ± 4 μmol/kg for CO_3^{2-}. These random errors represent ≈25% of the mean seasonal amplitude. Systematic errors are potentially introduced because of sparse seasonal sampling of carbon and hydrographic measurements, particularly during winter. We use independent carbon measurements obtained during winter months to verify the applicability of our empirical predictions (see *SI Text*). The meridional structure and magnitude of our predicted CO_3^{2-} compare well to these independent wintertime observations up to 70°S, with the distinctive CO_3^{2-} minimum being captured in the observations and predictions (see Fig. S2). It is important to note, however, that our empirical methodology seems to overestimate wintertime CO_3^{2-} close to the Antarctic continent (>75°S) because of nonexistent wintertime carbon data near the Antarctic continental shelf. It is therefore important to be aware that the results presented here for the Antarctic continental shelves will overestimate CO_3^{2-} during the winter and therefore not accurately capture the period to which aragonite undersaturation will occur in these regions.

Southern Ocean CO_2 Disequilibrium and Atmospheric CO_2 History. The model used here is the Commonwealth Scientific and Research Organization (CSIRO) ocean carbon cycle model (36, 37) and is used to determine the CO_2 disequilibrium for the future calculations. A CO_2 disequilibrium exists because the upper ocean lags the increase in atmospheric CO_2. The lag occurs because of both a finite rate of air–sea exchange of CO_2 and the ventilation of the upper ocean with older deep water, which contains lower anthropogenic CO_2. The CO_2 disequilibrium was determined from the year 1995 to the year 2100 (Fig. 3) and added to the observed annual cycle of pH and carbonate ion when determining future oceanic conditions. For clarity, we use the single IPCC IS92a scenario to estimate the onset of future aragonite undersaturation. We find that aragonite undersaturation is likely to begin once atmospheric CO_2 reaches ≈450 ppm, and the year at which this is reached will depend entirely on future anthropogenic CO_2 emission trajectories.

ACKNOWLEDGMENTS. This study would not have been possible without the efforts of those responsible for collecting and analysing Southern Ocean carbon parameters during WOCE and making those measurements available. B.I.M. was supported by a Queen Elizabeth II research fellowship from the Australian Research Council. R.J.M. would like to acknowledge the funding and support of CSIRO Wealth from Ocean Flagship and the Australian Climate Change Science Program. We would also like to thank Bob Key for technical support and assistance in the analysis of the Southern Ocean carbon database.

1. Caldeira K, Wickett ME (2003) Anthropogenic carbon and ocean pH. *Nature* 425:365–365.
2. McNeil BI, Matear RJ (2007) Climate change feedbacks on future oceanic acidification. *Tellus Ser B Chem Phys Meteorol* 59:191–198.
3. Orr JC, *et al.* (2005) Anthropogenic ocean acidification over the twenty-first century and its impact on calcifying organisms. *Nature* 437:681–686.
4. Fabry VJ, Seibel BA, Feely R, Orr JC (2008) Impacts of ocean acidification on marine fauna and ecosystem processes. *ICES J Mar Sci* 65:414–432.
5. Raven J (2005) *Ocean acidification Due to Increasing Atmospheric Carbon Dioxide* (Royal Soc, London).
6. Feely RA, *et al.* (2004) Impact of anthropogenic CO_2 on the $CaCO_3$ system in the oceans. *Science* 305:362–366.
7. Iglesias-Rodriguez MD, *et al.* (2008) Phytoplankton calcification in a high-CO_2 world. *Science* 320:336–340.
8. McNeil BI, Metzl N, Key RM, Matear RJ, Corbiere A (2007) An empirical estimate of the Southern Ocean air-sea CO_2 flux. *Global Biogeochem Cycles* 21, GB3011, doi:10.1029/2007GB002991.
9. McNeil BI, Matear RJ, Tilbrook B (2001) Does carbon 13 track anthropogenic CO_2 in the Southern Ocean? *Global Biogeochem Cycles* 15:597–613.
10. Follows MJ, Dutkiewicz S, Ito I (2006) On the solution of the carbonate system in ocean biogeochemistry models. *Ocean Modell* 12:290–301.
11. Kleypas JA, *et al.* (1999) Geochemical consequences of increased atmospheric carbon dioxide on coral reefs. *Science* 284:118–120.
12. Key RM, *et al.* (2004) A global ocean carbon climatology: Results from Global Data Analysis Project (GLODAP). *Global Biogeochem Cycles* 18, GB4031, doi:10.1029/2004GB002247.
13. Hopkins TL (1987) Midwater food web in McMurdo Sound, Ross Sea, Antarctica. *Mar Biol* 89:197–212.
14. Boysenennen E, Hagen W, Hubold G, Piatkowski U (1991) Zooplankton biomass in the ice-covered Weddell Sea, Antarctica. *Mar Biol* 111:227–235.
15. Hunt BPV, PakhoMoVab EA, Trotsenko BG (2007) The macrozooplankton of the cosmonaut sea, east Antarctica (30 degrees E-60 degrees E),1987–1990. *Deep-Sea Res Part I Oceanogr Res Pap* 54:1042–1069.
16. Cabal JA, *et al.* (2002) Mesozooplankton distribution and grazing during the productive season in the Northwest Antarctic Peninsula (FRUELA cruises). *Deep-Sea Res Part Ii Top Stud Oceanogr* 49:869–882.
17. Honjo S (2004) Particle export and the biological pump in the Southern Ocean. *Antarct Sci* 16:501–516.
18. Collier R, *et al.* (2000) The vertical flux of biogenic and lithogenic material in the Ross Sea: Moored sediment trap observations 1996–1998. *Deep-Sea Res Part Ii Top Stud Oceanogr* 47:3491–3520.
19. Honjo S, Francois R, Manganini S, Dymond J, Collier R (2000) Particle fluxes to the interior of the Southern Ocean in the Western Pacific sector along 170 degrees W. *Deep-Sea Res Part Ii Top Stud Oceanogr* 47:3521–3548.
20. Hunt BPV, Pakhomov EA, Hosie G, Siegel V, Ward P, Bernard K (2008) Pteropods in Southern Ocean ecosystems. *Progress in Oceanography* 78:193–221.
21. Gannefors C, *et al.* (2005) The Arctic sea butterfly Limacina helicina: Lipids and life strategy. *Mar Biol* 147:169–177.
22. Siebel BA, Dierssen HM (2003) Cascading trophic impacts of reduced biomass in the Ross Sea, Antarctica: Just the tip of the iceberg? *Biol Bull* 205:93–97.
23. Hunt BPV, Hosie GW (2006) The seasonal succession of zooplankton in the Southern Ocean south of Australia, part I: The seasonal ice zone. *Deep-Sea Res Part I Oceanogr Res Pap* 53:1182–1202.
24. Merico A, Tyrrell T, Cokacar T (2006) Is there any relationship between phytoplankton seasonal dynamics and the carbonate system? *J Mar Syst* 59:120–142.
25. Tyrrell T, Schneider B, Charalampopoulou A, Riebesell U (2008) Coccolithophores and calcite saturation state in the Baltic and Black Seas. *Biogeosciences* 5:485–494.
26. Feely RA, Sabine CL, Hernandez-Ayon JM, Ianson D, Hales B (2008) Evidence for upwelling of corrosive "acidified" water onto the continental shelf. *Science* 320:1490–1492.
27. Bates NR, Pequignet AC, Sabine CL (2006) Ocean carbon cycling in the Indian Ocean: 1. Spatiotemporal variability of inorganic carbon and air-sea CO_2 gas exchange. *Global Biogeochem Cycles* 20, GB3020, doi:10.1029/2005GB002491.
28. McNeil BI, Matear RJ, Key RM, Bullister JL, Sarmiento JL (2003) Anthropogenic CO_2 uptake by the ocean based on the global chlorofluorocarbon data set. *Science* 299:235–239.
29. McNeil BI, Tilbrook B, Matear RJ (2001) Accumulation and uptake of anthropogenic CO_2 in the Southern Ocean, south of Australia between 1968 and 1996. *J Geophys Res Oceans* 106:31431–31445.
30. Slansky CM, Feely RA, Wanninkhof R (1996) The stepwise linear regression method for calculating anthropogenic CO_2 invasion into the North Pacific. in *Biogeochemical Processes in the North Pacific*, ed Tsunogai S (Japan Marine Science Foundation, Aomori, Japan).
31. Wallace DWR (1995) Monitoring global ocean inventories. (Texas A and M, College Station), p 54.
32. Jabaud-Jan A, Metzl N, Brunet C, Poisson A, Schauer B (2004) Interannual variability of the carbon dioxide system in the southern Indian Ocean (20 degrees S-60 degrees S): The impact of a warm anomaly in austral summer 1998. *Global Biogeochem Cycles* 18, GB1042, doi:10.1029/2002GB002017.
33. Metzl N, Tilbrook B, Poisson A (1999) The annual fCO(2) cycle and the air-sea CO2 flux in the sub-Antarctic Ocean. *Tellus Ser B Chem Phys Meteorol* 51:849–861.
34. Millero FJ, Lee K, Roche M (1998) Distribution of alkalinity in the surface waters of the major oceans. *Mar Chem* 60:111–130.
35. Dickson AG, Millero FJ (1987) A comparison of the equilibrium-constants for the dissociation of carbonic-acid in seawater media. *Deep-Sea Res Part I Oceanogr Res Pap* 34:1733–1743.
36. Hirst AC, Gordon HB, Ofarrell SP (1996) Global warming in a coupled climate model including oceanic eddy-induced advection. *Geophys Res Lett* 23:3361–3364.
37. Matear RJ, Hirst AC (1999) Climate change feedback on the future oceanic CO2 uptake. *Tellus Ser B Chem Phys Meteorol* 51:722–733.
38. Orsi AH, Whitworth T, Nowlin WD (1995) On the meridional extent and fronts of the Antarctic circumpolar current. *Deep-Sea Res Part I Oceanogr Res Pap* 42:641–673.